Journal of
Geophysical Research

VOLUME 77 OCTOBER 10, 1972 NUMBER 29

Soil Mechanical Properties at the Apollo 14 Site

JAMES K. MITCHELL,[1] LESLIE G. BROMWELL,[2] W. DAVID CARRIER III,[3]
NICHOLAS C. COSTES,[4] AND RONALD F. SCOTT[5]

The Apollo 14 lunar landing provided a greater amount of information on the mechanical properties of the lunar soil than previous missions because of the greater area around the landing site that was explored and because a simple penetrometer device, a special soil mechanics trench, and the modularized equipment transporter (Met) provided data of a type not previously available. The characteristics of the soil at shallow depths varied more than anticipated in both lateral and vertical directions. While blowing dust caused less visibility impairment during landing than on previous missions, analysis shows that eroded particles were distributed over a large area around the final touchdown point. Measurements on core-tube samples and the results of transporter track analyses indicate that the average density of the soil in the Fra Mauro region is in the range of 1.45 to 1.60 g/cm^3. The soil strength appears to be higher in the vicinity of the site of the Apollo 14 lunar surface experiments package, and trench data suggest that strength increases with depth. Lower-bound estimates of soil cohesion give values of 0.03 to 0.10 kN/m^2, which are lower than values of 0.35 to 0.70 kN/m^2 estimated for soils encountered in previous missions. The in situ modulus of elasticity, deduced from the measured seismic-wave velocity, is compatible with that to be expected for a terrestrial silty fine sand in the lunar gravitational field.

Studies of the soil (regolith) at the Apollo 14 site have been made (1) to obtain data on the compositional, textural, and mechanical properties of lunar soils and the variations of these properties with depth and location at and among Apollo landing sites; (2) to use these data to formulate, verify, or modify theories of lunar history and lunar processes; (3) to develop information that may aid in the interpretation of data obtained from other surface activities or experiments (e.g., lunar field geology, passive and active seismic experiments); and (4) to develop lunar-surface models to aid in the solution of engineering problems associated with future lunar exploration. The in situ characteristics of the unconsolidated lunar-surface materials can provide an invaluable record of the past influences of time, stress, and environment on the moon. Of particular importance are particle size, particle shape, particle-size distribution, density, strength, and compressibility, and the variations in these properties both regionally and locally.

To date it has been necessary to rely heavily on observational data, such as are provided by photography, astronaut commentary, and ex-

[1] Department of Civil Engineering, University of California, Berkeley, California 94720.
[2] Department of Civil Engineering, Massachusetts Institute of Technology, Cambridge, Massachusetts 02139.
[3] Geophysics Branch, Planetary and Earth Sciences Division, Manned Spacecraft Center, NASA, Houston, Texas 77058.
[4] George C. Marshall Space Flight Center, Huntsville, Alabama 35812.
[5] Division of Engineering and Applied Science, California Institute of Technology, Pasadena, California 91109.

Copyright © 1972 by the American Geophysical Union.

amination of returned lunar samples, since quantitative data sources are limited. Semiquantitative analyses are possible, however, as *Costes et al.* [1969] showed for Apollo 11 and *Scott et al.* [1970] showed for Apollo 12. Such analyses are enhanced through terrestrial simulation studies [*Costes et al.*, 1971; *Mitchell et al.*, 1971].

The results of the Apollo 11 and 12 missions have generally confirmed the lunar-surface soil model developed by *Scott and Roberson* [1968]; that is, the lunar soil is similar to a silty fine sand, is generally gray-brown in color, and exhibits a slight cohesion. Evidence of both compressible and incompressible deformation has been observed. The lunar soil erodes under the action of the exhaust of the lunar module descent engine during lunar landing, kicks up easily under foot, and tends to adhere to most objects with which it comes into contact. The value (or range of values) of the in situ bulk density of the lunar soil remains uncertain, although Apollo 11 and 12 core-tube data and core-tube simulations [*Carrier et al.*, 1971] suggest a range of 1.5 to 1.9 g/cm^3 for the upper few tens of centimeters of the lunar surface.

Observations at five Surveyor landing sites and the Apollo 11 and 12 landing sites indicated relatively little variation in surface soil conditions with location. Core-tube samples from the Apollo 12 mission exhibited a greater variation in grain-size distribution with depth than had been found for Apollo 11 core-tube samples, however.

The Apollo 14 mission provided a greater amount of soil mechanics data than either of the previous missions for two reasons. The crew covered a much greater distance during the extravehicular activity periods, and the Fra Mauro landing site represented a topographically and geologically different region of the moon. In addition, three features of particular interest to soil mechanics were new to the Apollo 14 mission: the Apollo simple penetrometer, the soil mechanics trench, and the modularized equipment transporter (Met). Each of these has been used to shed new light on lunar soil characteristics.

APOLLO 14 LANDING SITE

The Apollo 14 landing site in the Fra Mauro region of the moon contains exposed geological formations that are characteristic of the Fra Mauro formation. This extensive geological unit is distributed in approximately radially symmetric fashion around the Sea of Rains over much of the near side of the moon and is considered to be older than the Apollo 11 and 12 mare sites. It is believed, also, that some of the material accessible at the site has come from depths of tens of kilometers within the original lunar crust. Bright ray material from Copernicus Crater covers much of the landing site. Cone Crater, a young, blocky, crater of Copernican age, 340 meters in diameter, penetrates the soil layer east of the landing point. The Apollo 14 traverses and a map of the major geologic features are shown in Figure 1.

DESCENT AND LANDING

Blowing dust. The astronauts commented that blowing dust was first observed at an altitude of approximately 33 meters and that the quantity of dust from that altitude down to the surface seemed less than had been encountered during the Apollo 11 and 12 landings. The crew estimated the thickness of blowing dust to be less than 15 cm; rocks were readily visible through it. The sun angle at landing was higher for the Apollo 14 mission than it had been for the Apollo 12 landing. The appearance of the blowing lunar-surface material in motion pictures taken during the Apollo 14 descent seems qualitatively similar to that observed during the Apollo 11 landing. Dust was first observed at altitudes of 24, 33, and 33 meters for the Apollo 11, 12, and 14 landings, respectively. Because of the effect of sun angle and spacecraft orientation, however, the appearance of the dust in the motion pictures may not be a reliable indication of the quantity of material removed from the surface.

Surface erosion. The astronauts reported that the lunar surface gave evidence of the greatest erosion in an area approximately 1 meter southeast of the region below the engine nozzle, where as much as 10 cm of surface material may have been removed during the landing. A distinct erosional pattern is visible in Figure 2. Except for a disturbed area in the left middle distance, the surface gives the appearance of having been swept by engine gases in the same way as on previous missions. The disturbed area may have developed as a conse-

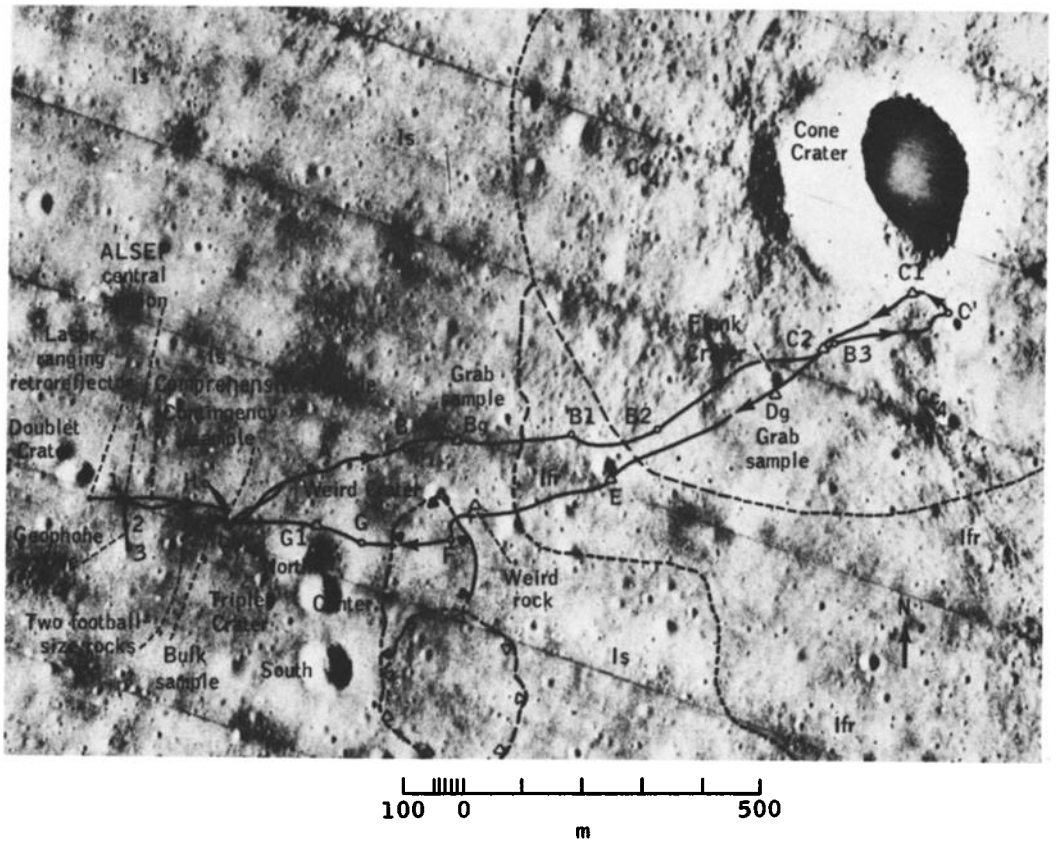

Fig. 1. Apollo 14 site map [from *Swann et al.*, 1971]: Cc_4, materials of Cone Crater; *Is*, smooth terrain material of the Fra Mauro formation; *Ifr*, ridge material of the Fra Mauro formation; open circle, panorama station; open triangle, station without panorama. *Contact:* long dashed lines indicate approximate locations, and short dashed lines indicate that location is inferred without local evidence. *Foot of scarp:* the line bounds a small mesa, and the solid triangles point downslope; the short dashed lines indicate inferred location. *Edge of hill:* long dashed lines indicate approximate locations, and short dashed lines indicate inferred location. The open triangles point downslope. Traverse routes for first and second periods of extravehicular activity are marked by solid lines with arrows.

quence of grazing contact of the $+Y$ footpad contact probe during the landing.

In the Apollo 14 descent motion pictures, it is evident that the lunar surface remains indistinct for a number of seconds after descent-engine shutdown. This event was probably caused by venting from the soil of the exhaust gas stored in the voids of the lunar material during the final stages of descent. The outflowing gas carries with it fine soil particles that obscure the surface.

Implications of blowing dust. The lunar soil removed by the engine exhaust gas is ejected radially from the surface below the spacecraft at predominantly low angles to the horizontal. There is thus, during the descent, a region from which soil is being removed, and an adjacent region, kilometers in lateral extent, on which the ejected particles descend. Since the spacecraft traverses laterally over the surface at a decreasing altitude, erosion in some regions will be followed by deposition of particles removed at later times from other areas.

The entire region in the vicinity of the landed spacecraft to a radius of several hundred meters is particularly subject to this process, which

Fig. 2. Area below the descent-engine nozzle showing erosional features caused by the exhaust gas. The $-Y$ footpad can be seen in the distance (AS14-66-9262).

may have some implications in the analyses of the soil and rock samples collected. The special environmental sample obtained from material in the bottom of the trench dug at station G (Figure 1) may be used as an example. It is likely that this soil sample included granular fragments both from below the surface and at the surface, since material fell into the trench as it was being excavated.

During descent to its landed position, the lunar module followed a track approximately W22°N, going slightly south of the center of North Crater. The spacecraft was about 60 meters (200 feet) south of station G at its point of closest approach, and at this point its altitude above the lunar surface was 55 meters (180 feet). Station G is slightly south of due east of the landing site at a distance of about 230 meters (750 feet). In the descent movie, the first signs of blowing dust are visible as the spacecraft passed over North Crater. Consequently, a small amount of erosion took place at station G as the spacecraft passed by during descent. This erosion is probably not significant to the analysis of the special environmental sample. However, the amount of material removed from the sur-

face increases greatly as the spacecraft descends, and major quantities are eroded from the landing site.

The concentration of particles arriving at station G and originating from the landing site can be estimated by comparison with the observations of the Apollo 12 mission. The Apollo 12 lunar module landed 155 meters (510 feet) from the Surveyor 3 spacecraft, which at the time had been on the lunar surface 31 months. Detailed study of the Surveyor 3 camera revealed a distinct shadow pattern on the paint, and this pattern was shown [*Jaffe*, 1971] to arise from a lunar soil sand blasting. It was demonstrated, moreover, that the sand-blasting particles came from the Apollo 12 landing site rather than from a sequence of points along its landing track. The particles must have had a velocity greater than about 70 meters per second with a shallow angle trajectory to have reached the Surveyor spacecraft and must have arrived at a fairly high concentration to have achieved the sharpness of shadow effect observed. The abrasion appears to be uniform, and there is no indication of individual impacts. Therefore, the surface or surface coating has been struck by so many particles that their impact areas overlap. It will be assumed that the majority of particles reaching Surveyor were of micrometer size or larger and that the average diameter of each impact might be of the order of 10 μm. If it is further assumed that the area of impacts just saturates the surface (conservative), it appears that each square centimeter of the abraded area was subjected to impact by about 10^6 particles. One of us (Scott) has examined the Surveyor 3 surface sampler (also exposed to blowing dust) in detail at about 100 magnification, at which he should certainly have been able to see any impact marks in the size range of order 100 μm, but there were none. Therefore, it can be tentatively concluded that each square centimeter of the Surveyor camera saw at least 10^4 particle impacts from the material eroded by the descent engine.

As a check, it is found that these numbers correspond to removal of the lunar soil to a depth of 3 or 4 cm over a diameter of 5 meters from the lunar surface below the descent engine nozzle. This is compatible with astronaut observations.

Station G is about 230 meters from the landed position of the Apollo 14 lunar module. If it is assumed that the Apollo 12 and Apollo 14 vehicles eroded identical quantities of lunar soil in the final stages of touchdown and that the emitted particle cloud expands spherically, the density of the particle cloud at station G would be $(155/230)^3 = 0.3$ of that at the Surveyor 3 location. Consequently, it would appear that each square centimeter of surface at right angles to the unobstructed line joining station G to the landing site would receive of the order of 10^3 impacts of particles, a few microns or more in diameter, ejected from the landing site. To reach station G, the particle velocities would need to be of the order of 100 m/sec or greater, depending on their ejection angle.

Footpad-surface interaction. The $-Y$ (Figure 2) and $-Z$ footpads penetrated the surface only to a depth of 2 to 4 cm, whereas the $+Y$ and $+Z$ footpads penetrated to a depth of 15 to 20 cm. The $+Y$ footpad penetration mechanism is clearly visible in Figure 3; the footpad contacted and plowed into the rim of a 2-meter-diameter crater. The motion of the footpad through the soil caused a buildup of a mound of soil on the north side of the pad. The $+Z$ footpad also landed on the rim of a small crater, and its appearance and penetration were similar to the appearance and penetration of the $+Y$ footpad.

The response of the soil to the landing (which occurred with little or no shock-absorber stroking) and the appearance of the soil in the footpad photographs suggest that the mechanical properties are similar to the mechanical properties of the lunar material on which the Apollo 11 and 12 lunar modules landed. The penetration of the $+Z$ and $+Y$ footpads caused the lunar module to tilt 1° to 1.5° in the westerly and northerly directions. Consequently, at the landing site, the strike of the lunar surface slope is approximately W16°N, and the dip is approximately 5.5° in the direction N16°E.

SOIL CONDITIONS AT THE LANDING SITE

The behavior of the surface soil was in many respects similar to that observed during earlier missions. The color was gray-brown and appeared to change with sun angle. The soil could be kicked up easily during walking, but would also compress under foot. Footprints ranged in

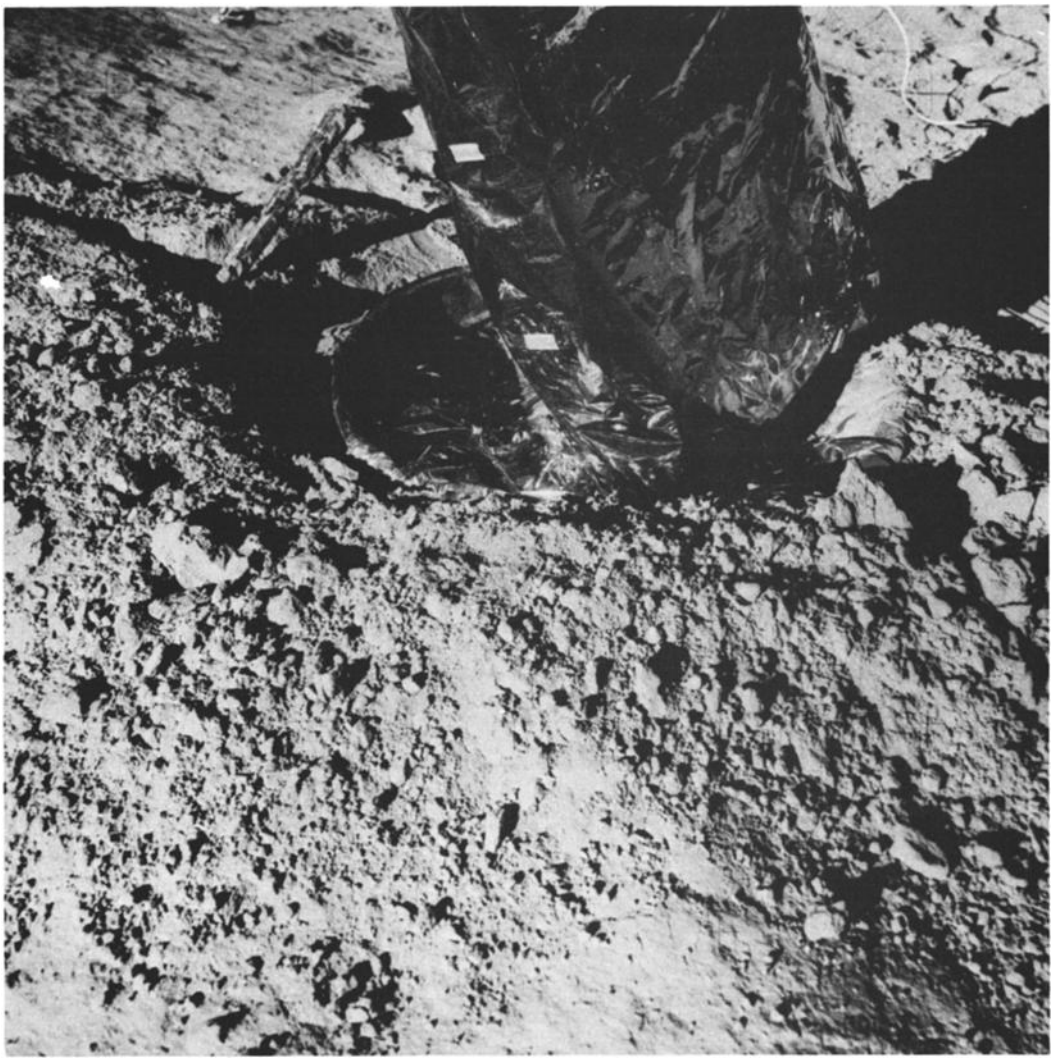

Fig. 3. The $+Y$ footpad embedded in the lunar soil. The gold foil surrounding the landing leg is probably the protective wrapping on the transporter (AS14-66-9234).

depth from 1 to 2 cm on level ground to 10 cm on the rims of fresh, small craters. The transporter tracks averaged 1 cm and ranged up to 8 cm in depth.

Patterned ground ('raindrop' pattern) was fairly general, except near the top of Cone Crater. The reason for the development of this surface texture is not yet known, although it is probably related to the impact of small particles on the lunar surface.

Crater morphologies range from fresh through subdued to almost completely obliterated. Determinations of minimum crater sizes associated with blocky ejecta [*Swann et al.*, 1971] lead to estimates of thickness of the soil layer in the Fra Mauro region ranging from 10 to 20 meters. Data from the active seismic experiment [*Kovach et al.*, 1971] indicate an unconsolidated surficial layer 8.5 meters thick at the site of the Apollo lunar surface experiments package (Alsep).

Surface characteristics are markedly different within a zone extending outward about 350 meters from the rim of Cone Crater from what they are elsewhere. In this region, the soil is coarse grained, and rock fragments are abun-

dant; elsewhere the soil is fine grained, and rock fragments are sparsely distributed on the surface.

The crew reported a zone of firm, compact soil between stations B1 and B2 (Figure 1) but said that this was a small, isolated patch in a generally powdery surface. Downslope movement of loose soil has obliterated some small craters on slopes.

As has been observed during previous missions, disturbed areas appear darker than undisturbed areas. Smoothed and compressed areas (e.g., transporter tracks and astronaut footprints) are brighter at some sun angles, as is shown in Figure 4. In some instances, it was difficult for the astronauts to distinguish between small, dust-covered rocks and clumps or clods of soil. The tops of many of the large rocks were free of dust, although fillets of soil were common around the bottom. The astronauts commented that the major part of most large rocks appeared to be buried beneath the

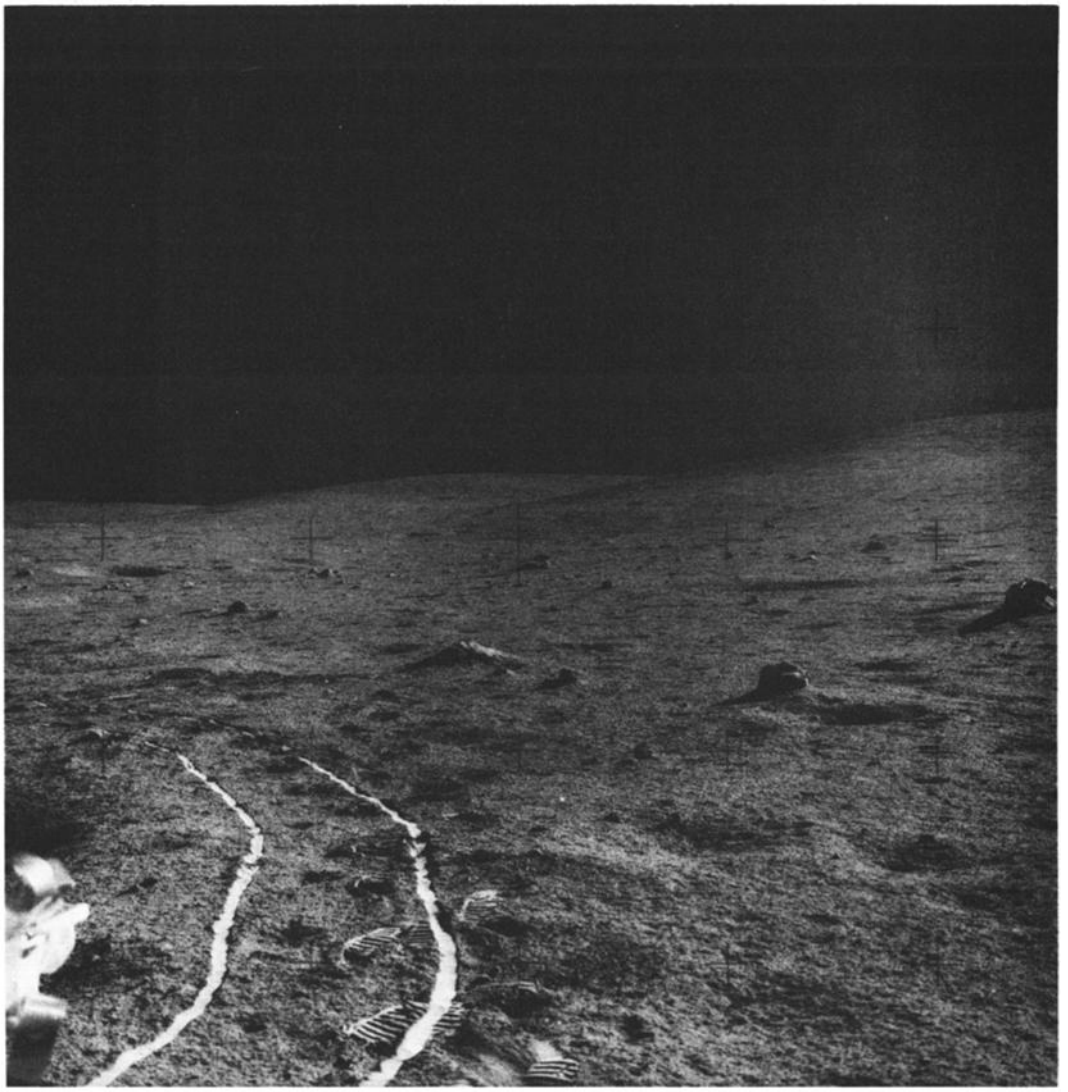

Fig. 4. The transporter tracks on relatively level, firm soil in the vicinity of station B during the second extravehicular activity (AS14-64-9058).

surrounding lunar surface. They also saw no obvious evidence of natural soil-slope failures on crater walls.

CHARACTERISTICS OF RETURNED SOIL SAMPLES

Nearly 14 kg of fines (soil) were returned from the lunar surface. In addition, two single and one double core-tube samples were obtained. Some observations relative to the physical and compositional characteristics of these materials are useful for subsequent interpretation of the mechanical properties of the soil in situ.

Physical characteristics. The soil from the Fra Mauro site is generally lighter in color and shows more color variability than that from the Apollo 11 and 12 sites. The color is more brown than black, probably because there is more plagioclase in the Apollo 14 soil than in earlier samples. Thus far, a significant proportion of glass beads has not been found, although the content of angular glass fragments is high.

The Apollo 14 bulk sample appears to be less cohesive than the soil from previous Apollo sites, even after removal of the fraction coarser than 1 mm by sieving. Whether this lesser cohesion reflects coarser grain-size distribution, different composition, or the effects of prolonged exposure to atmosphere is not yet known.

Grain-size distribution. Grain-size distributions for several samples are shown in Figure 5. Ranges in distribution for Apollo 12 samples are shown for comparison. It can be seen that the bulk sample, which is composed of surface and near-surface material, and the surface layer from the trench have particle sizes comparable to those of the Apollo 12 samples. However, material that fell out of the Cone Crater core sample and the material from the lower layer of the trench are considerably coarser, although still somewhat finer than the coarse layer found in the Apollo 12 double core tube [*Lindsay*, 1971]. Median grain sizes for the samples shown in Figure 5 are summarized in Table 1.

Core-tube samples. A double core-tube sample was obtained at station A (Figure 1). Near the rim of Cone Crater at station C′, an attempt to take a single core tube in a rock-strewn area failed when the soil sample (some or all) fell out of the core tube. At Triplet Crater (station G), two attempts to recover a triple core sam-

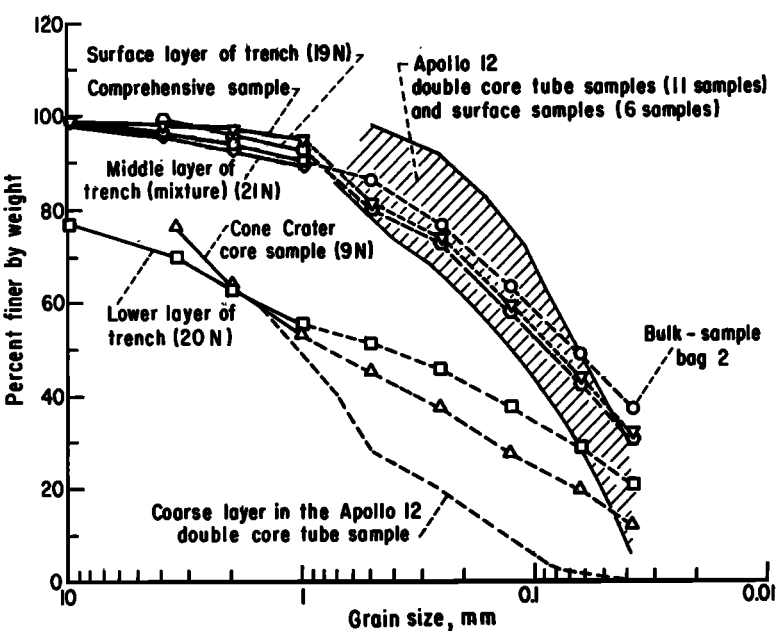

Fig. 5. Lunar soil grain-size distributions for several Apollo 12 and 14 samples. Apollo 14 sieve analyses were performed by the *Lunar Sample Preliminary Examination Team* [1971]. The solid parts of the Apollo 14 curves are for large samples (50 to 8000 grams), and the dashed parts are for small (<1-mm) subsamples (0.036 to 0.113 gram) of the large samples.

TABLE 1. Median Grain Sizes of Apollo 14 Soil Samples

Sample	Location[a]	Median Grain Size, mm
Comprehensive	Lunar module, upper 1 cm	0.050
Bulk sample, bag 2	Lunar module	0.065
Cone crater core	Station C'	0.735
Surface of trench	Station G	0.087
Middle of trench	Station G	0.068
Bottom of trench	Station G	0.410

[a]See Figure 1.

ple failed, and two single core-tube samples were obtained instead. In the first attempt for a single core tube, the astronaut reported that he had struck rock and had been unable to penetrate deeper than one core tube. Examination of the stainless steel bit from the core tube confirmed this, because it was visibly dented and burred. A second attempt was made approximately 9 meters north at a site that appeared similar. The coarseness of the soil at depth in this area, as revealed by the sample from the trench bottom, could account for the driving difficulties. Data on the returned core-tube samples are summarized in Table 2.

Data on the core tubes thus far available [*Mitchell et al.*, 1971; *Lunar Sample Preliminary Examination Team*, 1971; *Carrier et al.*, 1972] indicate:

1. The double core-tube sample contains from seven to nine layers ranging from 1 to 13 cm thick. Grain sizes appear to increase from top to bottom.

2. The single core-tube sample from Triplet Crater contains at least three layers, ranging in thickness from 0.5 to 5 cm.

3. The calculated bulk densities in the upper and lower halves of the double core tube (1.73 and 1.75 g/cm^3) are significantly less than the values of 1.98 and 1.96 g/cm^3 determined by *Carrier et al.* [1971] for the Apollo 12 double core-tube samples. Similarly, the bulk density for the single core tube of 1.60 g/cm is less than the value of 1.74 g/cm^3 obtained for the Apollo 12 single core tube. According to *Carrier et al.* [1972], the Apollo 14 core-tube densities correspond to in situ densities on the lunar surface of 1.45 to 1.60 g/cm^3. These smaller values of density are possibly due to a lower effective specific gravity for the Apollo 14 soil particles, which consist of more microbreccias and fewer

TABLE 2. Data on Apollo 14 Core-Tube Samples

Location	Sample Weight, grams	Sample Length, cm	Density in Tube, g/cm^3	Core Recovery, %	Estimated Density In Situ,[a] g/cm^3
Station A[b]	39.5	7.5[f]	1.73	63	1.60
Station A[c]	169.7	31.9[f]	1.75		
Station G[d]	80.7	16.5[f]	1.60	>49	1.45
Station G[e]	76.0	12.5[f]			

[a]*Carrier et al.* [1972].
[b]Upper part of double core tube.
[c]Lower part of double core tube.
[d]Single core tube near Triplet crater.
[e]Single core tube near Triplet crater; loose and undisturbed sample.
[f]Determined by *Heiken* [1971] by X radiography.

crystalline fragments than the Apollo 12 soil particles.

4. Some of the sample from Cone Crater may have mixed with the sample from Triplet Crater, because the same tube was used at both locations.

Soil composition. The results of studies by the *Lunar Sample Preliminary Examination Team* [1971] have established that the Apollo 14 soil samples vary in composition, as well as in grain size. The fractions containing particles finer than 1 mm have the following characteristics:

1. From less than 10% to 75% of the different samples are composed of glass.

2. There are abundant glass and lithic fragments in the coarser part of the <1-mm fraction, but the finer part is dominated by mineral particles.

3. Plagioclase and pyroxene are the most abundant, the plagioclase to pyroxene ratios varying from 16:1 to 1:2. This ratio varies both from sample to sample and from one size fraction to another. Some olivine is present.

4. Highly angular glass fragments finer than 62.5 μm in diameter are present, and there are only a few glass spheres.

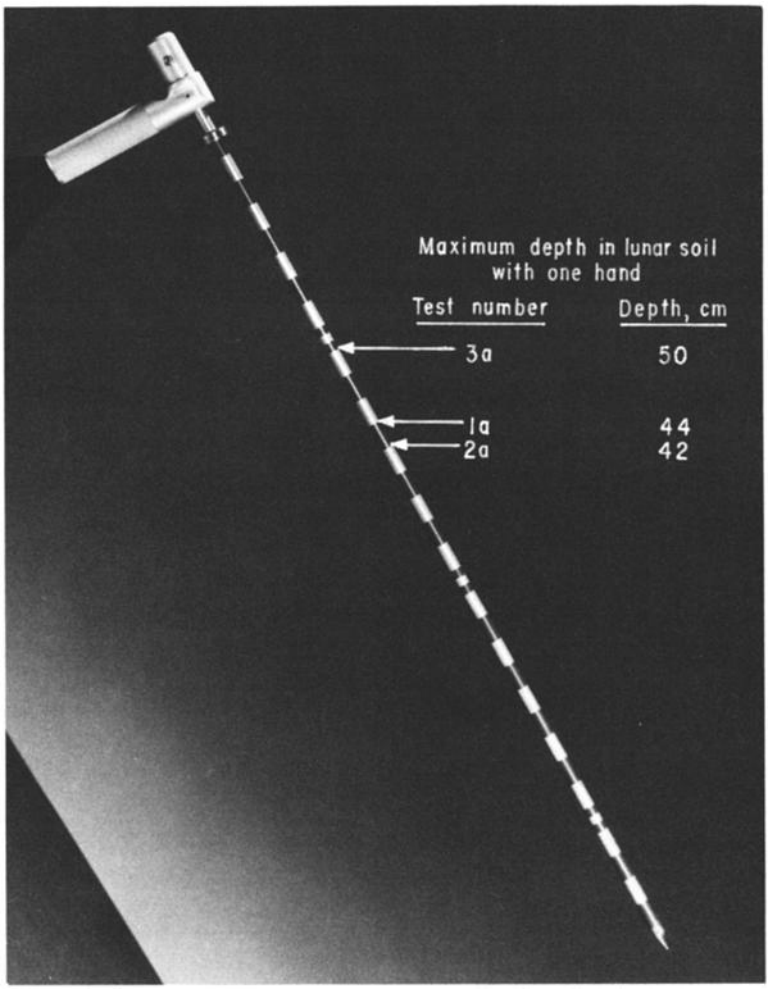

Fig. 6. Apollo simple penetrometer. The pilot pushed the penetrometer into the lunar soil three times. The arrows indicate the maximum depths he achieved while pushing with one hand. The full black-and-white strips are each 2 cm long (S-70-34922).

Lithic fragments, similar to the lithic clasts found in the fragmental rock samples, comprise 70 to 100% of the 1- to 2-mm fraction of the soil. Most of the rocks and soil samples closely resemble each other chemically.

ADHESIVE AND COHESIVE CHARACTERISTICS

Objects brought into contact with the lunar surface or with flying dust tended to become coated, although the layer generally remained thin. The equipment transporter sprayed dust around; however, thick layers did not form on any of the component parts, and no 'rooster tail' dust plume was noted behind the transporter wheels.

Although dust adhered readily to the astronauts' suits, it could be brushed off easily, except for that part that had been rubbed into the fabric. Dust sprinkled onto the thermal degradation sample array was easily brushed off, although that part of the dust that filled in the recessed number depressions of the sample tended to cohere. In this case, the dust formed into the pattern of the numbers; then, when the sample was tapped, the dust remained intact and bounced out of the depression, retaining the shape of the depression.

That the surface soil at the Fra Mauro site possesses a small cohesion is demonstrated in several ways; for example:

1. Clumping of soil in the vicinity of the lunar module footpads and elsewhere.
2. The numbers formed by dust on the thermal degradation sample.
3. Retention of deformed shapes and near-vertical slopes in astronaut footprints and transporter tracks.

It appears, however, that the cohesion is less than would be anticipated from the results of previous missions, as is noted subsequently. The source of lunar soil cohesion has not yet been determined; however, there are several possibilities: e.g., primary valence bonding between freshly cleaved surfaces, electrostatic attraction, and bonding through absorbed layers.

PENETRATION RESISTANCE OF THE LUNAR SURFACE

At the Alsep site in Figure 1, the Apollo simple penetrometer was used to obtain 3 two-stage penetrations into the lunar surface, thus providing information on soil property variations with depth. The lunar module pilot first pushed the penetrometer into the lunar soil as far as possible with one hand, called out the penetration depth, and then pushed it deeper with both hands. This procedure was repeated twice more at points approximately 4 meters apart.

A photograph of the penetrometer is shown in Figure 6. It can also be seen in the left middle of Figure 7, where it was later used as anchor for the geophone cable of the active seismic experiment. The penetrometer consists of a 68-cm-long aluminum shaft, which is 0.95 cm in diameter and has a 30° (apex angle) cone tip. The penetration depths are given in Figure 6 and Table 3. When the pilot pushed with both hands, no difficulty was experienced in penetrating deeper into the lunar surface, which indicates that the penetrometer had not struck a rock during the one-hand part of each test. The forces associated with the one-handed and two-handed modes shown in Table 3 were estimated from simulations performed by an experimenter in an astronaut's space suit flying in a 1/6-g trajectory in a KC 135 airplane.

The resistance of the lunar soil to penetration by the penetrometer consists of two components, point resistance and skin friction along the shaft:

$$F = F_p + F_s \tag{1}$$

where F is the lunar soil resistance, F_p is the point resistance, and F_s is the skin friction.

Both components are functions of soil strength, density, and compressibility and of frictional characteristics at the penetrometer-soil interface. Of the two types of resistance, point resistance is by far the more sensitive to variations in soil properties.

A general expression for skin friction is

$$F_s = f_s \pi D z \tag{2}$$

where f_s is the unit skin friction, D is the shaft diameter, and z is the penetration depth.

The unit skin friction is commonly calculated by using the equation

$$f_s = \gamma z K \tan \alpha \tag{3}$$

where γ is the unit weight of the soil, K is the coefficient of lateral earth pressure, and $\tan \alpha$

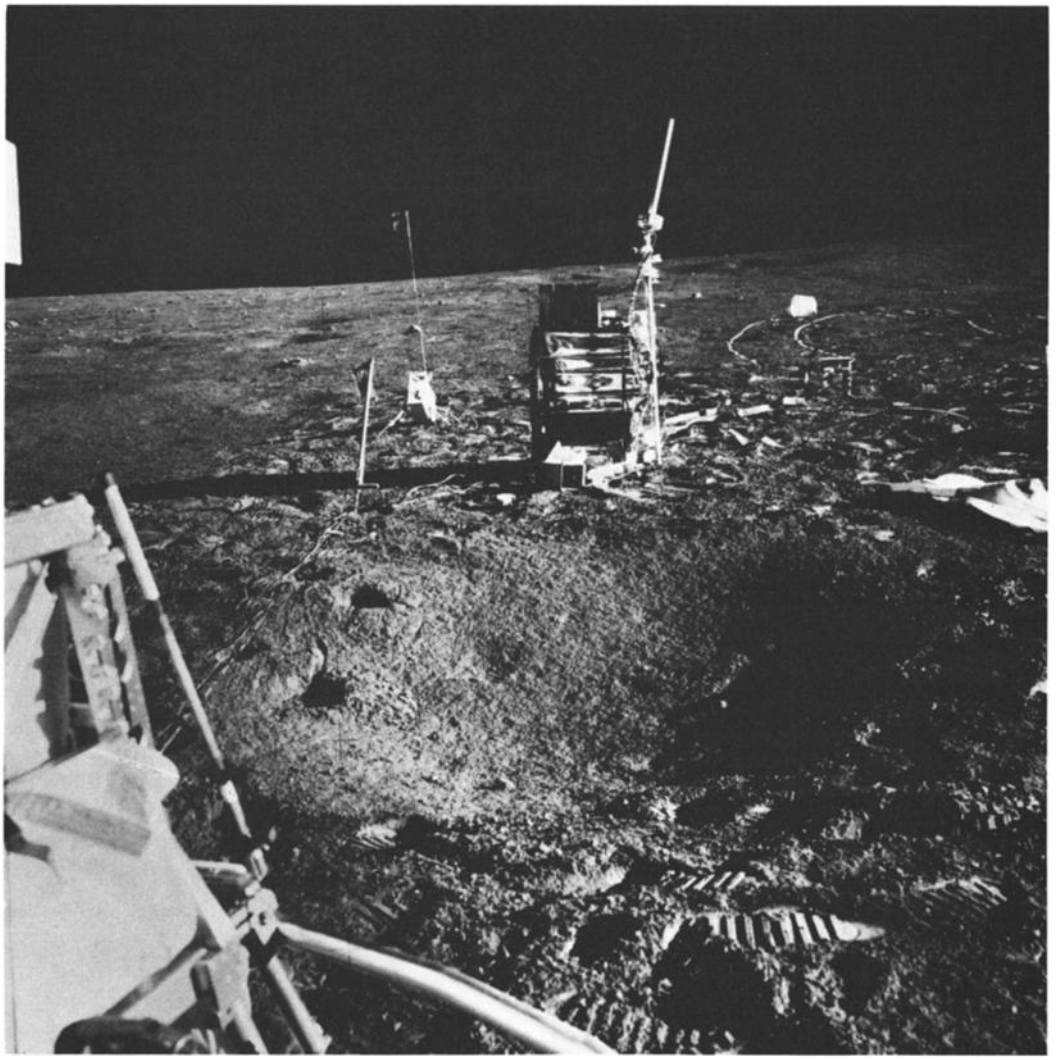

Fig. 7. The penetrometer, in position as anchor for the geophone cable, is shown in the left middle ground. Approximately 14 cm of the penetrometer shaft are visible above the lunar surface. The deep footprints and slope failures in the vicinity of the small crater in the foreground suggest softer soil in this area (AS14-67-9376).

is the coefficient of friction between the shaft and the soil.

Analysis of data by *Vesić* [1963] for cohesionless soils shows that actual unit-skin-friction values can be as much as five times greater than values calculated by using equation 3 and that a ratio of unit skin friction to unit point bearing of 0.3% is the least that can reasonably be assumed. If this were the case for the penetrometer measurements, a significant part of the applied force would have been carried by shaft friction. However, the value of F_s has also been investigated by laboratory simulations and has been found to be negligible compared with the uncertainty associated with the forces exerted by the astronaut. Thus, in the following analysis, values have been determined two ways: (1) $F_s = 0$, and (2) $f_s/(F_p/A) = 0.3\%$, where A is the penetrometer cross-sectional area.

Before Apollo 14, the strength of lunar soil had been determined quantitatively by direct in-place force-deformation measurements only by

TABLE 3. Apollo Simple Penetrometer Depths

Test	Depth z, cm	Mode of Force Application	Force F, N	Unit of Penetration Resistance F/A[a], N/cm^2
1*a*	44	One-Handed	71 to 134	100 to 188
1*b*	62	Two-handed	134 to 223	188 to 314
2*a*	42	One-handed	71 to 134	100 to 188
2*b*	68	Two-handed	<134 to 223	<188 to 314
3*a*	50	One-handed	71 to 134	100 to 188
3*b*	68	Two-handed	<134 to 223	<188 to 314

[a]Cross-sectional area of the penetrometer, 0.71 cm^2; all force is assumed to be carried in point bearing (F_s = 0).

means of the soil mechanics surface sampler experiment on Surveyors 3 and 7. On the basis of bearing-capacity theory for a shallow flat plate, *Scott and Roberson* [1968] calculated the following values.

Friction angle ϕ	37°–35°
Cohesion c	0.35–0.70 kN/m^2
Bulk density ρ	1.5 g/cm^3

While the bearing-capacity theory for an instrument like the Apollo simple penetrometer is not as well developed as that for a shallow flat plate, theory can be used to gain some insight into the shear-strength parameters of the soil in situ at the Apollo 14 landing site.

The point-bearing capacity of the penetrometer is given by

$$F_p/A = cN_c + \rho g z N_q \qquad (4)$$

where N_c and N_q are functions of friction angle ϕ, ρ is the soil density, and g is the acceleration of gravity.

A unique set of values of ϕ and c cannot be obtained from this equation, because there are three unknowns (c, ϕ, ρ). However, if a value of ρ is assumed, then for each value of ϕ there is only one value of c, and a curve of ϕ as a function of c can be calculated. This has been done in Figure 8 using a value of ρ = 1.8 g/cm^3 (variations in ρ have little effect on the calculations) and values for N_c and N_q (incom-

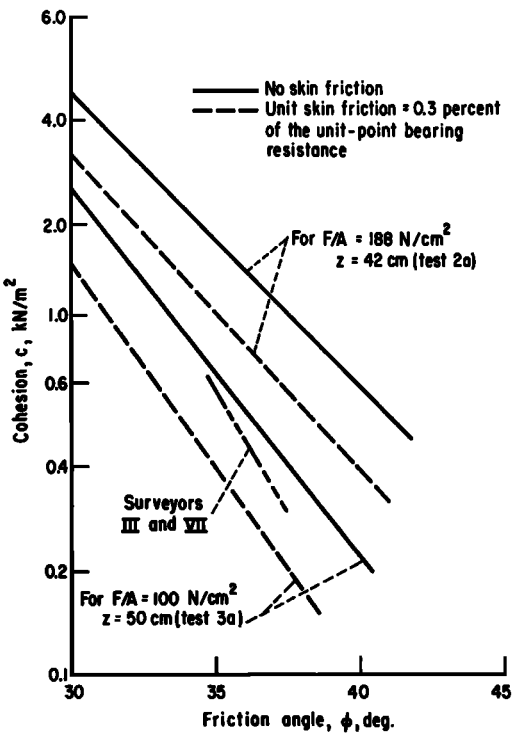

Fig. 8. Combinations of cohesion and friction angle to account for penetrometer resistance. The values of ϕ and c at the Apollo 14 Alsep site probably lie within the indicated bands. The parameters were calculated from the penetrometer data by means of the bearing-capacity theory.

pressible deformation assumed) from *Meyerhof* [1961, 1963]. The two cases ($F_s = 0$ and $f_s/(F_p/A) = 0.3\%$) noted above are shown.

The bands of values for ϕ as a function of c result from the range of depths for the three one-handed tests and from the uncertainty associated with the force applied by the astronauts (Table 3). The set of values for ϕ and c for the in situ soil at the Apollo 14 Alsep site must lie somewhere within these bands. Also plotted in Figure 8 is ϕ as a function of c for data from the Surveyor 3 and 7 sites. The band for the penetrometer parameters, if no skin friction is assumed, falls above and to the right of the Surveyor parameters, which implies that the values of the soil-strength parameters at the Apollo 14 landing site may be greater than those at the two Surveyor sites. However, if skin friction is a significant factor, the parameter values at the different landing sites may be approximately the same. The former situation is not unreasonable, however, because the Surveyor data are from surface tests, whereas the penetrometer data are from subsurface tests, and in general the lunar soil strength probably increases with depth.

The detailed variation of unit penetration resistance with depth in the lunar soil is probably very complex, as a result of layers and pockets in the soil with varying bulk density, grain-size distribution, cohesion, and other factors. An infinite number of possible distributions of unit penetration resistance as a function of depth would fit the penetrometer data obtained during the Apollo 14 mission, because only end-point values are known, although the pilot did indicate that penetration resistance increased with depth. Thus the data are insufficiently sensitive to reveal lateral inhomogeneities at depth among the three penetration sites.

Soil Mechanics Trench

At station G (Figure 1), Astronaut Shepard attempted to excavate a 60-cm-deep trench with one vertical sidewall to: (1) expose the in situ stratigraphy; (2) provide a means for estimation of soil-strength parameters by using stability analyses; (3) provide data on variations in soil texture and consistency; (4) enable sampling at depth, and (5) determine the ease with which surface material could be excavated.

The site chosen for trenching was the western rim of a small crater approximately 6 meters in diameter and 0.75 meter deep. A trenching tool consisting of a 21.6-cm-long (8.5-inch) by 15.2-cm-wide (6-inch) blade oriented at 90° to a handle was used like a backhoe by the astronaut. A view of the completed trench from the northeast is presented in Figure 9, which shows the steepest trench wall. Astronaut Shepard reported that digging was easy and estimated his first cut to be to a depth of approximately 15 cm with sidewalls at an angle of 70° to 80°. With the next cut, the walls were steepened to 80° to 85°, but at that point, they started caving. It is not clear from the various transcripts and debriefings just how steep the walls remained over-all, but it appears that, for the rest of the excavation, slopes steeper than approximately 60° could not be maintained.

The excavation passed through three distinct layers. The upper 3 to 5 cm were dark brown and fine grained. Next, a very thin layer (0.5 cm thick or less) of black glassy particles was encountered. Beneath this layer was a material much lighter colored and coarser grained. This stratification is not readily visible in Figure 9; however, the difference in grain size is marked, as is seen by the distribution curves in Figure 5 for samples from the upper and lower layers.

On the basis of previous estimates of lunar soil friction angle and cohesion at other sites, it was anticipated that trenching to a depth of 60 cm with near-vertical sidewalls should be possible without difficulty. If one assumes conservatively a homogeneous soil with a density of 1.9 g/cm^3, a cohesion of 0.35 kN/cm^2, and a friction angle of 35°, then a stability analysis indicates that a vertical cut should be possible to a depth of 85 cm before sidewall failure develops. Analysis of the Apollo 14 photographs shows a maximum trench depth in the range of 25 to 36 cm for sidewall slope angles increasing from 60° to 80°.

Combinations of cohesion c, density γ, slope height H, slope angle β, and friction angle ϕ that correspond to incipient failure for homogeneous slopes are shown in Figure 10. These curves are based on the assumption that curved (circular) failure surfaces pass through the toe of the slope and that soil is homogeneous. A band of values that probably encompasses the

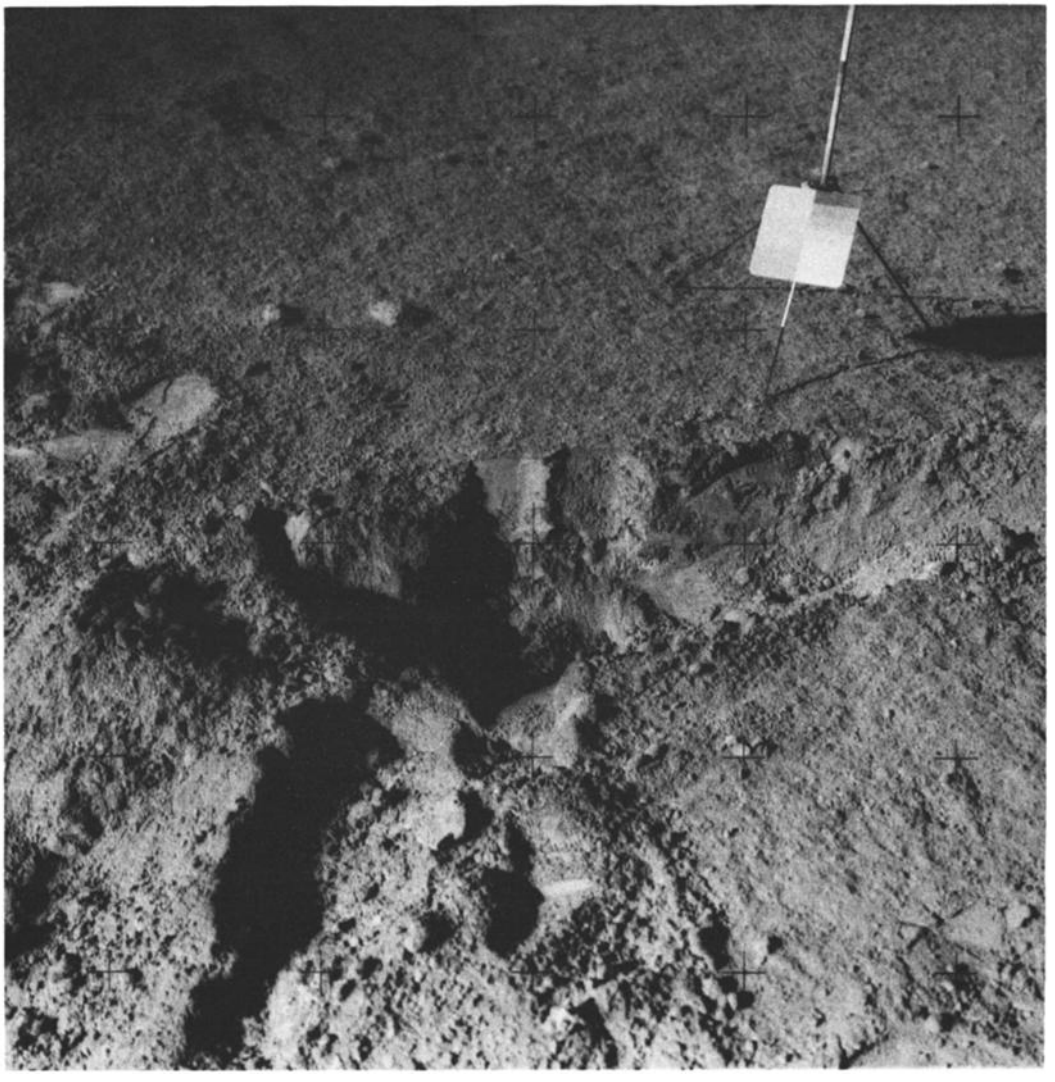

Fig. 9. View of the soil mechanics trench from the northeast. The steepest sidewalls are estimated to be 65° to 80°. A pile of excavated material is at the end of the trench at the left in the photograph (AS14-64-9161).

conditions in the Apollo 14 trench is shown in Figure 10.

For the slope angles and corresponding trench depths noted above, an assumed unit weight of 3 kN/m^3 in the lunar gravity field, and an assumed friction angle of 35°, the required cohesion values for stability fall in the range of approximately 0.03 to 0.10 kN/m^2. These values are considerably less than the values estimated using previous lunar-surface data. For higher values of friction angle, the values of cohesion required would be even less, as can be seen from Figure 10. It should be noted, however, that the computed values of cohesion are lower-bound estimates; that is, they are the minimum values required to maintain stability for the conditions shown. Nonetheless, it does appear that the soil beneath the surface at the location of the Apollo 14 trench is less cohesive than would have been anticipated on the basis of previous data. This lower value for cohesion is compatible with the coarser grain sizes encountered.

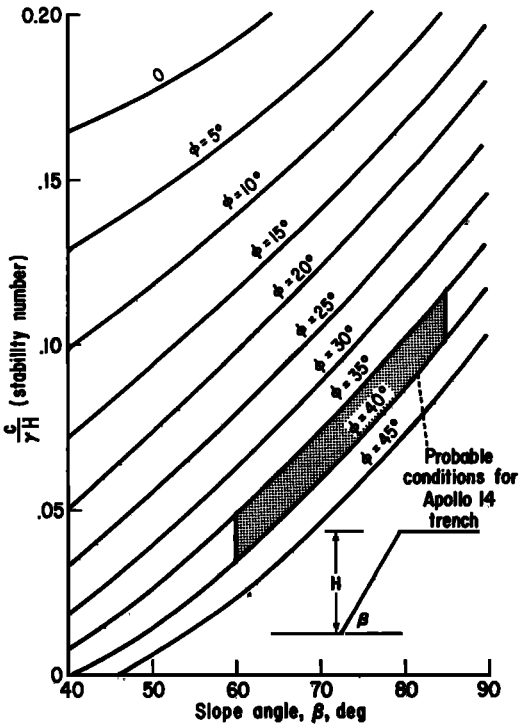

Fig. 10. Stability numbers for homogeneous slopes.

IN SITU PARTICLE-SIZE DISTRIBUTION

A preliminary analysis has been made to compare behavior during surface penetration and trenching with that predicted on the basis of the Apollo 11 and 12 particle-size distribution curves given by *Shoemaker et al.* [1969, 1970]. For the analysis, the assumptions have been made that particle-size distribution does not vary with depth and that the volumetric ratio of variously sized particles equals the area ratio observed at the surface, or

$$A_i/A_T = V_i/V_T \qquad (5)$$

where A_i is the area of particles of size i in the surface sample, A_T is the total surface area of the sample, V_i is the volume of particles of size i in the sample, and V_T is the total volume of the sample. Sufficient data are not available at present to determine reliably the probable variations in size-versus-frequency distribution with depth.

The total area of influence of all particles large enough to interfere with a penetrating probe was calculated. The influence area is given by

$$A_I = \sum_{i=i_c}^{i=n} \frac{\pi}{4}(D_i + D_p)^2 N_i \qquad (6)$$

where A_I is the total influence area of all particles larger than i_c, i_c is the smallest particle size that will stop penetration, D_i is the diameter of particle i, D_p is the diameter of the probe, and N_i is the number of particles in the size range i (850 size ranges were used to describe the Apollo 12 size-versus-frequency distribution curve).

The ratio of this influence area to the total sample area represents the probability of striking a critical particle in a unit volume. The analysis is conducted to any desired depth, and the cumulative probability of not encountering a critical obstructing particle is calculated.

The probability analysis was used to determine the likelihood that the three penetrometer penetrations could be made to the full depth of the instrument (68 cm) without encountering a rock equal to or larger than the diameter of the instrument (0.95 cm). The probability for the three events was calculated to be 51%.

The four core-tube events were analyzed in a similar manner. The combined probability of the four tubes being driven to their respective depths without encountering a fragment equal to or greater than the core-tube diameter (1.95 cm) was 67%. In fact, one of the core tubes (tube 2022) hit an obstruction. The probability that one or more core tubes would hit an obstruction was only 33%.

The Apollo 11 and 12 size distribution curves were also used to predict the number of particles of a given size that should be found in the soil mechanics trench. The results indicate that only a few particles larger than 1 cm would have been expected in the excavated soil. However, many rocks in the 1- to 2-cm range were reported, and numerous particles of this size can be observed in the photographs of the trench. Furthermore, the grain-size distributions determined in the Lunar Receiving Laboratory for material from the bottom of the trench (Figure 5) showed more than 20% of the sample to be coarser than 1 cm. This is strong evidence that the determinations of particle size versus frequency made at the surface of the Apollo 11 and 12 sites are not good indi-

cators of the size distributions likely to occur with depth at other sites.

LATERAL VARIATION OF SOIL PROPERTIES

Study of the variability of soil properties with lateral position is important in order to ascertain both the magnitude and randomness of the variations that may be encountered. It is of interest to know whether variations can be associated directly with differences in geomorphological features or whether the influences on the soil of original geomorphology may have been obliterated by random lunar-surface processes, as would be indicated by nearly random local variations and near homogeneity on a regional basis.

Variations in crater morphology at the Apollo 14 landing site indicate the following age sequence of craters along the geologic traverses (Figure 1), beginning with the oldest, according to interpretations by *Eggleton and Offield* [1970] and by *Trask* [1966] as reported by *Swann et al.* [1971].

1. Highly subdued craters characterized by very gentle depressions at (*a*) the landing site

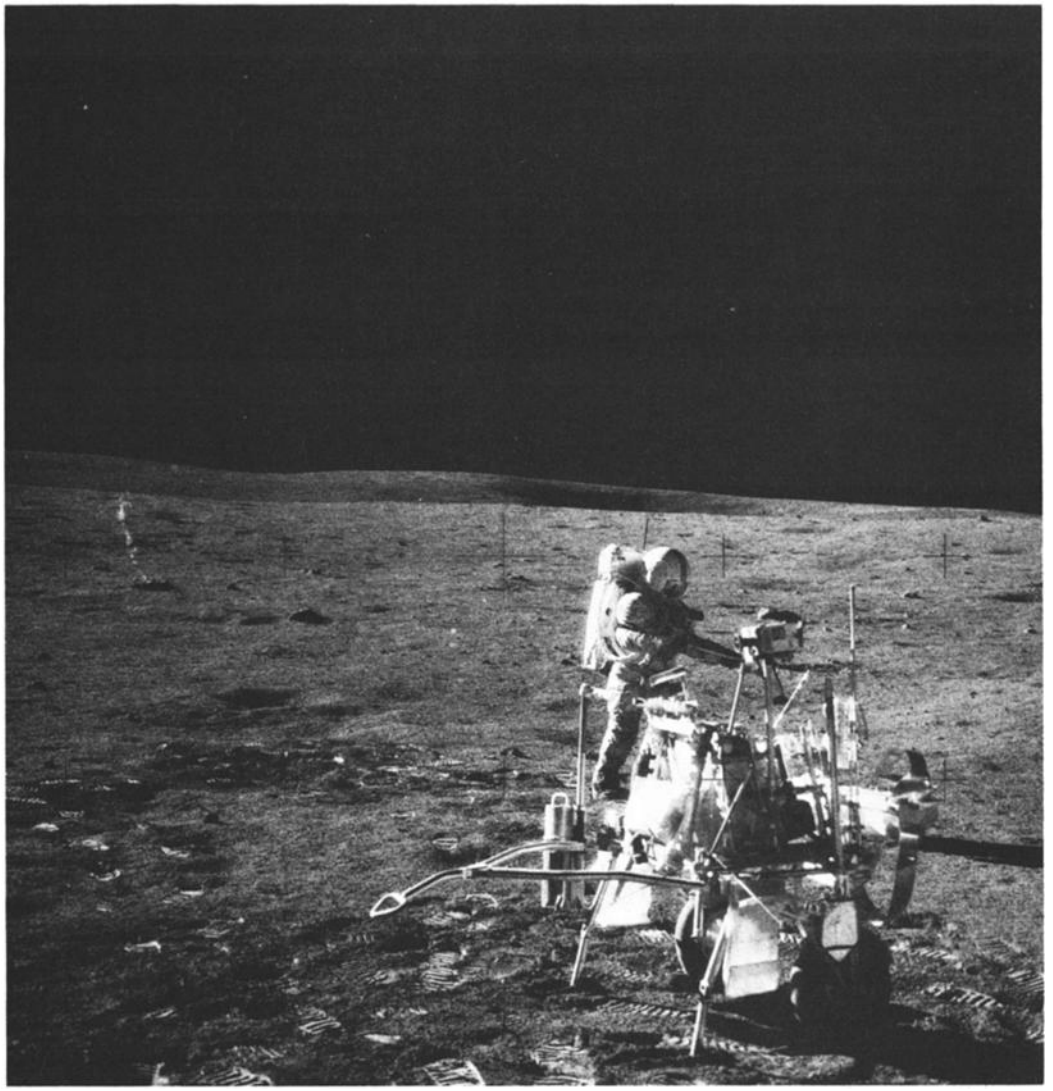

Fig. 11. The transporter in use during the second extravehicular activity (AS14-68-9404).

of the lunar module; (*b*) west of the lunar module at the Alsep deployment site; and (*c*) north of station A.

2. Moderately subdued craters at (*a*) North Triplet Crater; (*b*) the 50-meter-diameter crater east of station F; and (*c*) the 10-meter crater at station A.

3. Cone Crater and the sharp 45-meter crater at station E.

4. The sharp 300-meter crater at station C and a small 10-meter crater next to which a football-size rock was collected during the first extravehicular activity.

Information relating to soil properties associated with these features can be obtained by inference from the observed interaction of various objects of known geometry and physical characteristics with the lunar surface. One such type of interaction that has been useful for study of soil properties is that of the wheels of the modularized equipment transporter with the surface.

The transporter (Figure 11) is a two-wheeled, ricksha-type vehicle equipped with pneumatic tires that was used to carry equipment during both periods of extravehicular activity. The maximum weight of the vehicle plus payload in lunar gravity was 128 N (28.9 lb), including a maximum weight of rock and soil samples of 38.7 N (8.7 lb). During the second period of extravehicular activity, the transporter traversed a distance of approximately 2.8 km, and the total weight fluctuated between 89 and 120 N, depending on the amount of sample collected.

The transporter tracks in the vicinity of station B can be seen in Figure 4. The astronauts estimated the track depths to vary between 0.5 and 2 cm and noted that the largest sinkages occurred around soft crater rims. A closeup photograph of a transporter track in the immediate vicinity of station A is shown in Figure 12. The estimated track depth at this location is 1.0 cm.

The facts that the transporter was equipped with pneumatic tires of known geometry and load-deflection characteristics and that the lunar soil at the Apollo 14 site is predominantly granular make possible the estimation of the average change in the penetration resistance with depth, designated by G_L, on the basis of the analysis developed by *Freitag* [1965] for cohesionless soils. With this quantity known and the results of tests on lunar soil simulants, it has been possible to estimate the in-place void ratio e_L, density ρ_L, and friction angle ϕ_L for the soil on the moon. This procedure is described in the Appendix.

The results of the analysis are presented in Table 4. From the indicated ranges in lunar soil properties, it can be seen that within regions of comparable geologic age there is a small but distinct difference between average properties of soil located in intercrater areas on firm, level ground and soil located in soft pockets and fresh crater rims and slopes. No appreciable differences in lunar soil properties between regions of different geologic age are discernible, however, on the basis of the computed values.

It appears, therefore, that, within the upper few centimeters of the lunar surface at the Fra Mauro landing site, the initial consistency of the lunar soil resulting from a major geologic event of short duration, such as the primary impact of a large meteoroid or the impact of ejecta, has been modified by long-duration processes that have created a steady-state condition. Such processes may include the continuous flux of micrometeoroids and the steady downslope movement of material, superposed on the continuous formation and extinction of small and medium-size impact craters. The continuous interaction of such events with the lunar surface is further evidenced by the following observations: (1) formation of raindrop patterns on relatively level surficial fine-grained material, but low frequency of occurrence of such patterns on steeper slopes; (2) rounding off of boulders and development of fillet material against outward-sloping rock surfaces; and (3) the presence of small fine-grained hummocks a few centimeters in size. Irrespective of age, however, the lunar soil at the surface appears in general to be firmer at level intercrater areas than at small fresh crater rims and slopes.

LUNAR SOIL MODULUS

The results of the Apollo 14 active seismic experiment, reported by *Kovach et al.* [1971], indicated that the seismic velocity (*P* wave) in the upper 8.5 meters of the Fra Mauro site is 104 m/sec. According to elastic theory for a homogeneous, isotropic medium, the *P*-wave

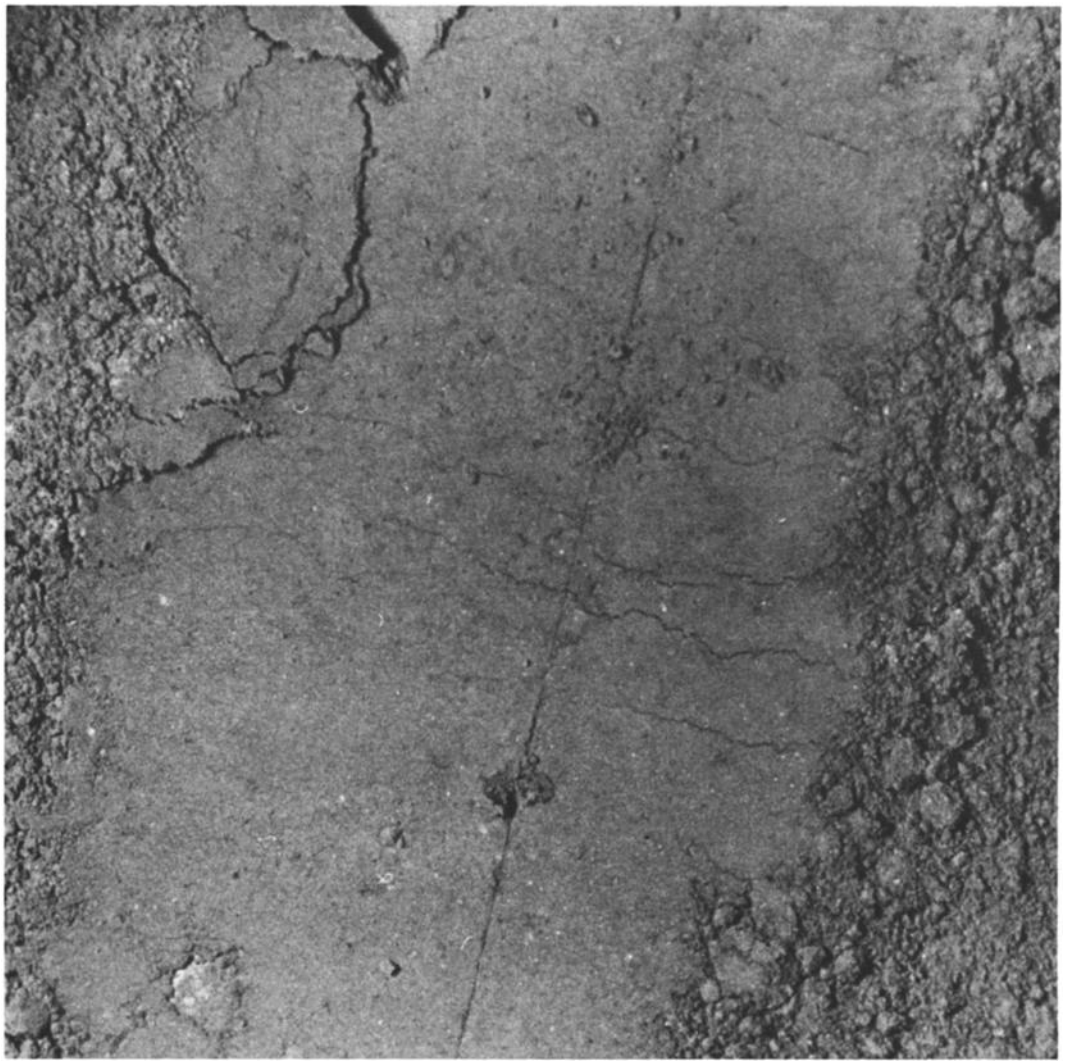

Fig. 12. Close-up photograph of transporter track in the vicinity of station A. The transporter has evidently rolled across slightly firmer soil, because the track narrows, indicating less sinkage. A small white rock has been pushed into the soil by the tire in the lower left-hand corner of the photograph. The indention at the upper left-hand corner of the photograph was probably produced by the edge of the camera while it was being pisitioned (AS14-77-10358).

velocity v_p is related to Young's modulus E by

$$v_p = \left[\frac{E(1-\nu)}{\rho(1+\nu)(1-2\nu)}\right]^{1/2} \quad (7)$$

where ρ is density, and ν is Poisson's ratio.

Combinations of modulus, density, and Poisson's ratio corresponding to a velocity of 104 m/sec are shown in Figure 13. From a number of studies on cohesionless terrestrial soils, it is known that Young' modulus at small deformation is related to confining pressure σ_3 according to

$$E = Kp_a(\sigma_3/p_a)^n \quad (8)$$

where K and n are parameters dependent on soil type, and p_a is terrestrial atmospheric pressure in the same units as σ_3. *Kulhawy et al.* [1969] have shown that for well-graded sands

TABLE 4. Variation in Lunar Soil Properties with Lateral Position as Determined From Transporter Tracks

Geology Traverse Stations[a]	Terrain Type	$G_{L'}$, N/cm^3	e_L	$\rho_{L'}$[b], g/cm^3	$\phi_{L'}$, deg
		Highly Subdued Craters			
Lunar module site	Level	0.83 to 0.47	0.68 to 0.70	1.85 to 1.81	43.4 to 41.0
Alsep site, sta. A, B	Firm	0.73	0.69	1.84	42.8
Lunar module site	Soft spots	0.34 to 0.27	0.74 to 0.75	1.79 to 1.77	39.6 to 38.5
	Crater rims	0.30	0.74	1.78	39.0
		Moderately Subdued Craters			
A, G, B_2	Level	2.02 to 0.47	0.62 to 0.71	1.91 to 1.81	47.1 to 41.0
	Firm	0.91	0.68	1.85	43.2
A, B_1, B_2	Soft spots	0.47 to 0.20	0.71 to 0.77	1.81 to 1.75	41.0 to 37.2
	Crater rims	0.30	0.75	1.77	38.5
		Sharp Craters			
B_3, C'	Level	0.83 to 0.34	0.68 to 0.74	1.85 to 1.79	43.4 to 39.6
	Firm	0.65	0.70	1.83	42.1
C'	Soft spots	0.47 to 0.20	0.71 to 0.77	1.81 to 1.75	41.0 to 37.4
	Crater rims	0.34	0.74	1.78	39.4

Values of lunar soil properties given as either ranges or averages.
[a]According to descending geologic age.
[b]These values of density are somewhat higher than those estimated on the basis of core-tube data (Table 2). They can be attributed in part to the value of 3.1 assumed for specific gravity in the analysis. The results of recent (1972, unpublished) tests on two Apollo 14 soil samples suggest that a value of 2.95 is more appropriate.

typical values of K and n are 300 and 0.50, respectively. From test data given by *Namiq* [1970] for a lunar soil simulant, n can be deduced to be 0.51, and K increases from 34 at a void ratio of 0.8 to 130 at a void ratio of 0.6.

From these values, one can compute average moduli corresponding to confinement at a depth of 4.25 meters on the lunar surface (half the depth of the estimated thickness of the unconsolidated layer). If the lateral pressure is taken as one-half the vertical pressure, probably a reasonable lower bound, the resulting modulus values are in the range of about 0.1×10^4 to 0.75×10^4 kN/m^2. It can be seen that these values fall within the range, but at the lower end, of those shown on Figure 13. There is reason to believe that, had the terrestrial measurements been carried out under high-vacuum conditions, the modulus values would have been somewhat higher owing to the absence of adsorbed films between particles.

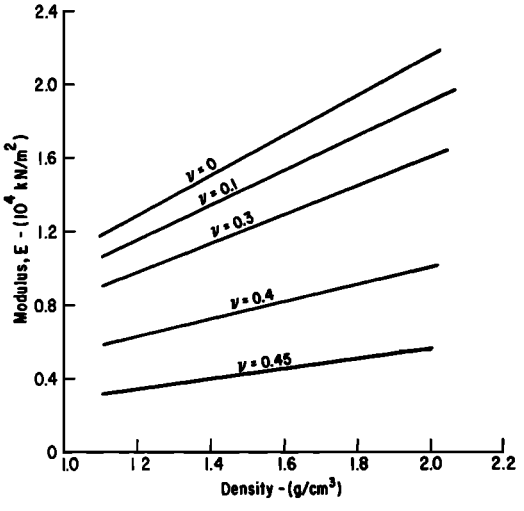

Fig. 13. Young's modulus as a function of density and Poisson's ratio for a seismic velocity of 104 m/sec.

The importance of these results is that special or unusual soil properties need not be assumed in order to account for the low seismic velocities. On the moon, the low-gravity conditions result in low confinement, which in turn gives a low seismic velocity.

CONCLUSIONS

The results of the Apollo 14 mission have provided new insights into the properties and behavior of the soil at the surface of the moon. Some of the more significant findings resulting from the analyses herein are as follows:

1. A greater variation exists in the characteristics of the soil at shallow depths (a few centimeters) in both lateral and vertical directions than had previously been supposed, and soil with a particle-size distribution in the medium- to coarse-sand range may be encountered at shallow depths.

2. There is evidence that venting from the soil voids of descent-engine exhaust gas after engine shutdown caused fine particle movement.

3. Particles eroded by the exhaust plume of the lunar module descent engine during landing were distributed over a large area around the final touchdown point.

4. As had been the case in previous missions, dust was easily kicked up and tended to adhere to any surface contacted.

5. Soil density determined from a double core-tube sample taken at station A was about 1.60 g/cm^3. These values are lower than those obtained from the Apollo 12 core tubes, but are well within the range thought to be characteristic of the moon over-all.

6. The results of simple penetrometer measurements suggest that the soil in the vicinity of the Apollo 14 Alsep may be somewhat stronger than soil at the landing sites of Surveyor 3 and 7, and comparison of the results of analyses using penetrometer, transporter-track, and trench data suggests that soil strength increases with depth.

7. Computations of soil cohesion at depth at the site of the soil mechanics trench result in lower-bound estimates considerably lower than were expected from the results of previous missions (0.03 to 0.10 kN/m^2 as opposed to 0.35 to 0.70 kN/m^2).

8. The determinations from the Apollo 11 and 12 sites of surface particle size versus frequency are not good indicators of the size distributions likely to occur with depth at other sites.

9. Analysis of transporter-track depths has indicated angles of internal friction in the range of 40° to 45° (if a cohesionless soil is assumed) for soil near the surface, and that the soil is less dense, more compressible, and weaker at the rims of small craters than in level intercrater regions.

10. The magnitude of the in situ modulus of elasticity, based on the measured seismic-wave velocity, is compatible with that to be expected for a terrestrial silty fine sand layer in the lunar gravitational field.

APPENDIX
DETERMINATION OF SOIL PROPERTIES FROM MET TRACK DATA

It is assumed that the functional relationships describing the tire-soil interaction under lunar environmental conditions and low velocities are essentially the same as the relationships describing the corresponding tire-soil interaction on earth. On this basis, the normalized sinkage z/d, in which z is the penetration depth of the tire and d is the tire diameter, is related to the dimensionless quantity

$$N_{SM} = \frac{G(bd)^{3/2}}{W}\frac{\delta}{h} \tag{9}$$

in which G is the average change of cone penetration resistance with depth, b is the tire section width, W is the tire load, δ is the tire deflection, and h is the tire section height, by the same function relationship as the corresponding quantities are related to sand under terrestrial environmental conditions.

The dimensionless quantity N_{SM}, termed the sand-mobility number by *Freitag* [1965], expresses the soil strength and density characteristics through the quantity G. The average penetration-resistance gradients G_L of the lunar soil at various locations along the geological traverse were determined using transporter-track depth data (estimated from Hasselblad camera stereo-pairs), known tire characteristics, and the z/d versus N_{SM} diagram shown in Figure 14. The solid curve represents the best fit for terrestrial wheel-soil interaction test data (180 tests) reported by *Green* [1967]. These tests were performed with pneumatic tires of different geometries and size on a uniform dune sand from the Arizona desert, designated Yuma sand. Figure 14 also shows wheel-soil interaction data obtained from tests performed with transporter tires inflated to the same pressure and subjected to the same load range as those on the lunar surface. A lunar soil simulant consisting of a crushed basalt, Waterways Experimental Station (WES) mix, was used for these tests.

Values of G_L (Table 4) determined from Figure 14 were converted to corresponding values in the earth's gravitational field G_E by assuming

that penetration resistance varies in direct proportion to gravity level; i.e., $G_E = 6\ G_L$, in accordance with the analysis of *Costes et al.* [1971].

The behavior of the lunar soil simulant and that of the actual lunar soil were assumed to be the same if both are at the same void ratio. Accordingly, G_E values were used to estimate the in-place lunar soil void ratios e_L (Table 4) at corresponding locations from the diagram of G versus void ratio for the lunar soil simulant (WES mix) shown in Figure 15. Corresponding values of soil density have been determined assuming that the specific gravity of the lunar soil particles averages 3.1.

Values of friction angle for different values of G and density were estimated as follows [*Costes et al.*, 1971]: The resistance to penetration of the lunar soil can be expressed by the *Terzaghi* [1943] simplified bearing-capacity equation for foundations:

$$q_z = s_c c N_c + \tfrac{1}{2} s_\gamma \rho g B N_\gamma + s_q \rho g z N_q \qquad (10)$$

where qz is the bearing capacity of the foundation (i.e., the resistance to penetration of the lunar soil at depth z), c is the soil cohesion, ρ is the bulk density of soil, g is the acceleration of gravity, B is the least dimension of foundation base (dimension of foundation), z is the vertical distance from the surface to the base of the foundation, N_c, $N\gamma$, N_q are bearing capacity factors that depend on the angle of internal friction ϕ of the soil, and s_c, s_γ, s_q are factors that depend on the shape of the foundation.

If it is assumed that c, N_c, ρ, $N\gamma$, and N_q are independent of depth, then from equation 10

$$dq_z/dz = S_q \rho g N_z$$

But, from the definition of G,

$$dq_z/dz = G$$

so that N_q can be found from

$$N_q = G/S_q \rho g \qquad (11)$$

Values of friction angle were determined, using equation 11 and N_q versus ϕ diagrams developed by *Meyerhof* [1961] for shallow conical-shaped foundations and are listed in Table 4.

It could be argued that the bearing-capacity factors N_c, N, and N_q will increase with depth, since the density of the soil will tend to increase with depth, and both the cohesion c and ϕ

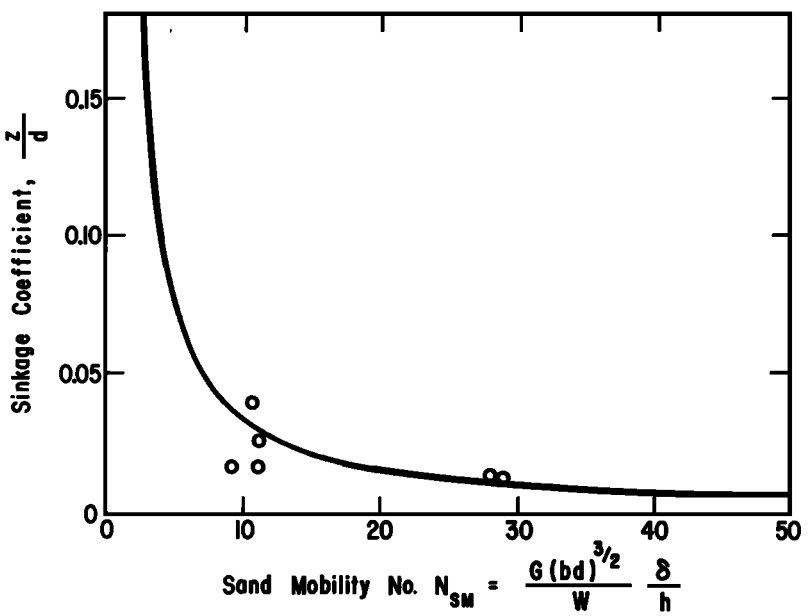

Fig. 14. Tire sinkage versus sand mobility number for two soils. The curve represents the best fit to first-pass tests on Yuma sand at Towed Point [*Green*, 1967]. The points represent first-pass tests with transporter tire on lunar soil simulant (WES mix) at Towed Point.

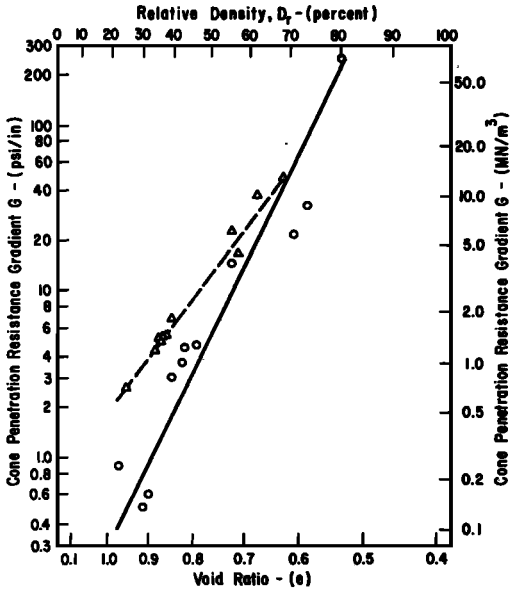

Fig. 15. Variation of penetration resistance gradient of lunar soil simulant (WES mix) with soil consistency and packing characteristics. The moisture content ω is 0.9% for the solid curve and 1.8% for the dashed curve.

increase with increasing density, and because the geometry of the zone of plastic equilibrium within the soil mass changes with depth. Because of this, the derivative of q_z in equation 10 with respect to z will not be as shown in equation 11, but in general will include additional terms as follows:

$$dq_z/dz = G = A + (B + S_q\rho N_q)g \qquad (12)$$

in which A and B are quantities independent of q and are obtained by differentiating c, ρ, ϕ, N_c, $N\gamma$, and N_q with respect to z. Thus the ratio G_r of the penetration-resistance gradient of the soil at 1-g gravity level to that for the same soil at 1/6-g gravity level is less than 6. This observation is corroborated by the analyses of *Houston and Nœmiq* [1971], who found that a ratio of 3 to 4 was appropriate for the lunar soil simulant used by them. The actual value in any case will be highly dependent on the magnitude of the cohesion contribution to the strength.

Within the range of G, e, and ϕ values estimated to be representative of the in-place properties of the lunar soil, the functional relation of G versus ρ or e of lunar soil simulants is such that ρ and e are not sensitive to the variations in G_E values that result by multiplying the corresponding G_L values by G_r ranging between 3 and 6. The relationship between N_q and ϕ is such that ϕ is not sensitive to the resulting variations in N_q given by equation 11. The ϕ values associated with G_r ranging between 3 and 4 are lower than the ϕ values resulting from taking $G_r = 6$ by 1 to 1½ deg. Corresponding variations in density are of the order of 2%.

Acknowledgments. Professor W. N. Houston, Dr. H. J. Hovland, and H. T. Durgunoglu assisted in simulation studies and data analyses at the University of California, Berkeley. Dr. Stewart W. Johnson, Richard A. Werner, and Ralf Schmitt participated in phases of the work carried out at the Manned Spacecraft Center, Houston. G. T. Cohron assisted in the transporter-track analyses, which were done at the Marshall Space Flight Center, Huntsville, Ala. The assistance of these individuals is gratefully acknowledged.

The studies reported herein were supported, in part, by NASA contract NAS 9-11266, principal investigator support for soil mechanics experiment (S-200), and NASA contract NAS 9-11454, co-investigator support for soil mechanics experiment (S-200).

REFERENCES

Carrier, W. D., III, S. W. Johnson, R. A. Werner, and R. Schmidt, Disturbance in samples recovered with the Apollo core tubes, in *Proceedings of the Second Lunar Science Conference*, vol. 3, pp. 1959–1972, MIT Press, Cambridge, Mass., 1971.

Carrier, W. D., III, S. W. Johnson, L. H. Carrasco, and R. Schmidt, Core sample depth relationships: Apollo 14 and 15, in *Proceedings of the Third Lunar Science Conference*, vol. 3, in press, MIT Press, Cambridge, Mass., 1972.

Costes, N. C., W. D. Carrier III, J. K. Mitchell, and R. F. Scott, Apollo 11 soil mechanics investigation, Apollo 11 Preliminary Science Report, *NASA Spec. Publ. 214*, pp. 85–122, 1969.

Costes, N. C., G. T. Cohron, and D. C. Moss, Cone penetration resistance test: An approach to evaluating in-place strength and packing characteristics of lunar soils, in *Proceedings of the Second Lunar Science Conference*, vol. 3, pp. 1973–1987, MIT Press, Cambridge, Mass., 1971.

Eggleton, R. E., and I. W. Offield, Geologic maps of the Fra Mauro region of the moon, Map I-708, U.S. Geol. Survey, Washington, D.C., 1970.

Freitag, D. R., A dimensional analysis of the performance of pneumatic tires on soft soils; *Tech. Rep. 3-688*, 140 pp., U.S. Army Eng. Waterways Exp. Sta., Vicksburg, Miss., 1965.

Green, A. J., Development and evaluation of mobility numbers for coarse-grained soils, Performance of Soils under Tire Loads, *Tech. Rep. 3-666, 5,* U.S. Army Eng. Waterways Exp. Sta., Vicksburg, Miss., 1967.

Heiken, G., Apollo 14 core tubes, Memorandum to TN 12/Curator, Planet. and Earth Sci., NASA Manned Spacecraft Center, Houston, Tex., April 29, 1971.

Houston, W. N., and L. I. Namiq, Penetration resistance of lunar soils, *J. Terramech., 8,* 59–69, 1971.

Jaffe, L. D., Blowing on lunar soil by Apollo 12: Surveyor 3 evidence, paper presented at Second Lunar Science Conference, NASA, Houston, Tex., Jan. 11–14, 1971.

Kovach, R. L., J. S. Watkins, and T. Landers, Active seismic experiment, Apollo 14 Preliminary Science Report, *NASA Spec. Publ. 272,* chap. 7, pp. 163–174, 1971.

Kulhawy, F. H., J. M. Duncan, and H. B. Seed, Finite element analyses of stresses and movements in embankments during construction, *Rep. TE 69-4,* 169 pp., Geotech. Eng., Univ. of Calif., Berkeley, 1969.

Lindsay, J. F., Sedimentology of Apollo 11 and 12 lunar soils, *J. Sediment. Petrol., 41,* 780–797, 1971.

Lunar Sample Preliminary Examination Team, Preliminary examination of lunar samples, Apollo 14 Preliminary Science Report, *NASA Spec. Publ. 272,* chap. 5, pp. 109–132, 1971.

Meyerhof, G. G., The ultimate bearing capacity of wedge-shaped foundations, *Proceedings of the Fifth International Conference on Soil Mechanics and Foundation Engineering,* vol. 2, pp. 105–109, Dunod, Paris, 1961.

Meyerhof, G. G., Some recent research on the bearing capacity of foundations, *Can. Geotech. J., 1,* 16–26, 1963.

Mitchell, J. K., L. G. Bromwell, W. D. Carrier III, N. C. Costes, and R. F. Scott, Soil mechanics experiment, Apollo 14 Preliminary Science Report, *NASA Spec. Publ. 272,* chap. 4, pp. 87–108, 1971*a*.

Mitchell, J. K., W. N. Houston, T. S. Vinson, T. Durgunoglu, L. I. Namiq, J. B. Thompson, and D. D. Treadwell, Lunar surface engineering properties and stabilization of lunar soils, report, NASA contract NAS 8-21432, 223 pp., Space Sci. Lab., Univ. of Calif., Berkeley, 1971*b*.

Namiq, L. I., Stress-deformation study of a simulated lunar soil, Ph.D. thesis, 218 pp., Univ. of Calif., Berkeley, 1970.

Scott, R. F., and F. I. Roberson, Soil mechanics surface sampler, Surveyor Project Final Report, Part 2, *Tech. Rep. 32-1265,* pp. 195–207, Jet Propul. Lab., Pasadena, Calif., 1968.

Scott, R. F., W. D. Carrier III, N. C. Costes, and J. K. Mitchell, Mechanical properties of the lunar regolith, Apollo 12 Preliminary Science Report, *NASA Spec. Publ. 235,* pp. 161–182, 1970.

Shoemaker, E. M., N. G. Bailey, R. M. Batson, D. H. Dahlem, T. H. Foss, M. J. Grolier, E. N. Goddard, M. H. Hait, H. E. Holt, K. B. Larson, J. J. Rennilson, G. G. Schaber, D. L. Schleicher, H. H. Schmitt, R. L. Sutton, G. A. Swann, A. C. Waters, and M. N. West, Geologic setting of the lunar samples returned by the Apollo 11 mission, Apollo 11 Preliminary Science Report, *NASA Spec. Publ. 214,* pp. 41–84, 1969.

Shoemaker, E. M., R. M. Batson, A. L. Bean, C. Conrad, Jr., D. H. Dahlem, E. N. Goddard, M. H. Hait, K. B. Larson, G. G. Schaber, D. L. Schleicher, R. L. Sutton, G. A. Swann, A. C. Waters, H. E. Holt, J. J. Rennilson, R. F. Scott, W. D. Carrier III, N. C. Costes, and J. K. Mitchell, Preliminary geologic investigation of the Apollo 12 landing site, Apollo 12 Preliminary Science Report, *NASA Spec. Publ. 235,* pp. 113–182, 1970.

Swann, G. A., N. G. Bailey, R. M. Batson, R. E. Eggleton, M. H. Hait, H. E. Holt, K. B. Larson, M. C. McEwen, E. D. Mitchell, G. G. Schaber, J. B. Schafer, A. B. Shepard, R. L. Sutton, N. J. Trask, G. E. Ulrich, H. G. Wilshire, and E. W. Wolfe, Preliminary geologic investigations of the Apollo 14 landing site, Apollo 14 Preliminary Science Report, *NASA Spec. Publ. 272,* pp. 39–86, 1971.

Terzaghi, K., *Theoretical Soil Mechanics,* 510 pp., John Wiley, New York, 1943.

Trask, N. J., Size and spatial distribution of craters estimated from Ranger photographs: Rangers 8 and 9, *NASA Tech. Rep. 32-800,* pp. 252–263, 1966.

Vesić, A. B., Bearing capacity of deep foundations in sand, *Rep. 39,* pp. 112–153, Highway Res. Board, Nat. Res. Council, Washington, D.C., 1963.

(Received December 10, 1971;
revised June 15, 1972.)